Journal of Power Sources 378 (2018) 311–321

New Battery Model Considering Thermal Transport and Partial Charge Stationary Effects in Photovoltaic off-Grid Applications

Iván Sanz-Gorrachategui[a], Carlos Bernal[a], Estanis Oyarbide[a], Erik Garayalde[b], Iosu Aizpuru[b], Jose María Canales[b], Antonio Bono-Nuez[a]
a Departamento de Ingeniería Electrónica y Comunicaciones, Universidad de Zaragoza, Zaragoza, Spain
b Departamento de Electrónica, Mondragon Universitatea, Gipuzkoa, Spain

Abstract: The optimization of the battery pack in an off-grid Photovoltaic application must consider the minimum sizing that assures the availability of the system under the worst environmental conditions. Thus, it is necessary to predict the evolution of the state of charge of the battery under incomplete daily charging and discharging processes and fluctuating temperatures over day-night cycles.

Much of previous development work has been carried out in order to model the short term evolution of battery variables. Many works focus on the on-line parameter estimation of available charge, using standard or advanced estimators, but they are not focused on the development of a model with predictive capabilities. Moreover, normally stable environmental conditions and standard charge-discharge patterns are considered. As the actual cycle-patterns differ from the manufacturer's tests, batteries fail to perform as expected.

This paper proposes a novel methodology to model these issues, with predictive capabilities to estimate the remaining charge in a battery after several solar cycles. A new non-linear state space model is proposed as a basis, and the methodology to feed and train the model is introduced. The new methodology is validated using experimental data, providing only 5% of error at higher temperatures than the nominal one.

Keywords:

Battery Model

Storage system

Photovoltaic off-grid applications

Temperature fluctuation modelling

Incomplete charge modelling

1. Introduction

Small scale generation systems that use renewable sources are becoming popular in some specific applications, and almost all of them require the use of energy storage systems, usually battery packs. On the one hand battery packs are used to store energy and power the application during non-generation periods like, for example, night-time in Photovoltaic (PV) applications. On the other hand, the other main purpose when including batteries in small-scale generation systems is to mitigate the unforeseeable energy production rates that most renewable sources offer, such as cloudy or misty weather (PV application) or non-windy periods (wind application). In off-grid systems, these technologies are mainly based on electrochemical storage through batteries, using well-known chemistries such as Valve Regulated Lead-Acid (VRLA) batteries [1] and usually with stationary features.

When it comes to designing one of these Energy Storage Systems (ESS), engineers usually consider battery manufacturer's datasheets as their main tool for battery sizing purposes. Manufactures use laboratory experiments to characterize their batteries but in very specific conditions, e. g. fixed optimum test temperature, full-charge tests, etc. These controlled tests do not usually fit the real performance conditions of renewable energy applications (because of the unstable conditions concerning off-grid installations) and so, the results cannot be extrapolated. Moreover, in off-grid system applications these uncontrolled parameters have a huge impact on battery performance [2]. As there is almost no information about the influence of these variations, from manufacturer's tests to real applications, electrical engineers are forced to oversize the installation designs, as a measure to avoid energy supply disruption.

This study addresses how to model some of these uncontrolled effects in batteries related to off-grid PV sites. The main environmental variables that have an influence on this kind of installation are temperature and insolation. On the one hand, while temperature impact is measured by battery manufacturers over many cycles [3], temperature variations within the same cycle are not studied. On the other hand, regarding insolation, uncertainty exists regarding over time incomplete charge cycles, and the decrease in effective battery capacity that they produce. As a previous work to this paper, these issues have been described in [4], and are not usually modeled together.

Nowadays, there is an increasing interest in the research of battery models (mainly boosted by their use in the Electric Vehicle application (EV) and on-grid ESS). These technologies are mainly specialized in cycling capabilities, such as batteries based on Lithium-Ion or ultracapacitors [5]–[7]. This fact has caused an increase in battery modelling effort in literature, but unfortunately, simulation of off-grid PV ESS applications is not the main aim of these studies. The modelling techniques that have been proposed can be mainly classified into on-line estimation algorithms [8] or off-line simulation models [9], and are mainly focused in diagnosing performance parameters throughout the battery use, such as estimating State-Of-Charge (SOC) [10], [11], or service life (State-Of-Health, SOH) [12], [13].

Moreover, most studies are usually addressed in nominal temperature conditions (20ºC or 25ºC) where batteries perform best, omitting the huge impact that temperature has on features like capacity or degradation. If considered, temperature is mostly addressed as a static variable, omitting temperature changes within the same cycle [14], [15]. Hence there is also uncertainty regarding the impact of charge–discharge cycles in non-constant temperature environment [4]. Being deployed in remote, isolated locations, off-grid PV ESS applications are greatly affected by this specific kind of thermal cycles, which have an important impact on charge estimators and energy management policies.

Additionally, in off-grid PV applications battery packs suffer from incomplete charge cycles. When testing a battery in a laboratory, manufacturers use complete charge processes to measure the battery capacity. During these tests, batteries are kept in float stage for several hours, typically 72h [3], [16], [17] and can be considered fully charged prior to the test. Once discharged, all the energy is drawn from them. However, in a real ESS with one battery pack in an off-grid PV application, batteries cannot remain in that stage so many hours, since batteries are discharged during the night. This incomplete charge processes leads to a steady partial charge state, as described in [4] that lowers the effective available charge for non-generation periods.

Coming ESS generations will include more than one energy storage packs, and there will be an increasing number of publications related to energy management policies, which control the power flow inside the ESS. In order to simulate these behaviors and to develop new intelligent policies, a well fitted battery simulation model will be needed.

This paper proposes a new battery model intended for off-grid PV applications, which is able to make long-term predictions, and not only short-term estimations based on past or real-time data. The model introduces a novel thermal transport estimation feature that considers charge and discharge processes at different temperatures within the same cycle. It is also capable of performing accurate estimations of the remaining charge inside a battery after several incomplete charge cycles with progressive temperature changes. The model performs long term predictions and performance simulations of ESS, being able to forecast SOC in off-grid PV applications with real world conditions In this paper, SOH is not taken into account, since it is not possible to evaluate its impact on battery performance in the short term, and its effects can be ignored in a short time window. Future work will deal with this issue, leading to a more complex model.

2. Methodology

Typically, batteries work in the Current Regulation Phase (the charger fixes the current through the battery) while charging. As the battery charges it voltage rises, until it reaches a value established as the float voltage. When this happens, the battery charger switches to Voltage Regulation Phase and the current that the battery draws decreases over time (current tail).

Furthermore, in this application (off-grid supplied telecom equipment), the load demands a constant current from the battery. This will be relevant when choosing inputs or outputs to the model.

2.1. Model Description

The aim of the battery model is to: a) replicate the battery charge over time, and b) provide the related voltage. When dealing with charge, the most widely used parameter is *SOC*. Many studies have addressed *SOC* estimation using different approaches [13]. Extended Kalman Filter (EKF) together with circuital modelling [18] is one of the most popular, intended for on-line estimation applications. Coulomb Counting (CC) is another approach [19] similar to State-Space (SS) modelling. The latter is the modelling approach retained in this paper.

2.1.1. Basic battery model

Before proceeding, some definitions are required:

- Q: represents the stored charge in the battery. This charge is obtained with the CC or SS method, by integrating the input current through the battery terminals.
- C_{NOM}: is the rated capacity of the battery, as specified by the manufacturer. Usually measured at 20ºC or 25ºC, and in full charge conditions.
- i_{batt}: represents the current that flows through the battery terminals.
- *SOC*: is the traditional definition of State-Of-Charge, obtained by comparing the stored charge Q with the rated capacity C_{NOM} as displayed in (1). The definition in (2) can be obtained applying the CC method. An alternative definition (SOC_V) will be used, as explained further [11].

$$SOC \triangleq \frac{Q}{C_{NOM}} \times 100\%; SOC \in [0,100] \qquad (1)$$

$$SOC(t) = \frac{1}{C_{NOM}} \int_{-\infty}^{t} i_{batt}(\tau) d\tau \qquad (2)$$

- *OCV*: is the Open Circuit Voltage of the battery, i.e. its voltage with no current flow through its terminals and once the relaxation of the battery is completed. It is related to the *SOC* by a non-linear relationship.
- v_{batt}: represents the voltage measured at the battery terminals, with or without current. *OCV* and v_{batt} are related by the battery output impedance model and i_{batt}.

A first hypothesis is made to formulate the model: Q is supposedly predictable, that is, considering the evolution of external variables of the system (current patterns, float voltage and temperature) it is possible to compute the evolution of Q. An

internal description through a SS model has been retained where the *SOC*, defined as in (1), represents a tentative State Variable, see Fig. 1.a. The basic model estimates *SOC* through the well-known method of CC (2). Input current integration is translated into the remaining charge inside the battery, which acts as a state variable.

The next step in the model is to establish the battery *OCV* as a result of the *SOC,* based on the measured charge-discharge curves. This first basic scheme models the electrochemical processes within the battery, which are complex and beyond the scope of this work. The basic model is completed with an electrical modelling of the dynamic behavior of the battery [20], see Fig. 1.b.

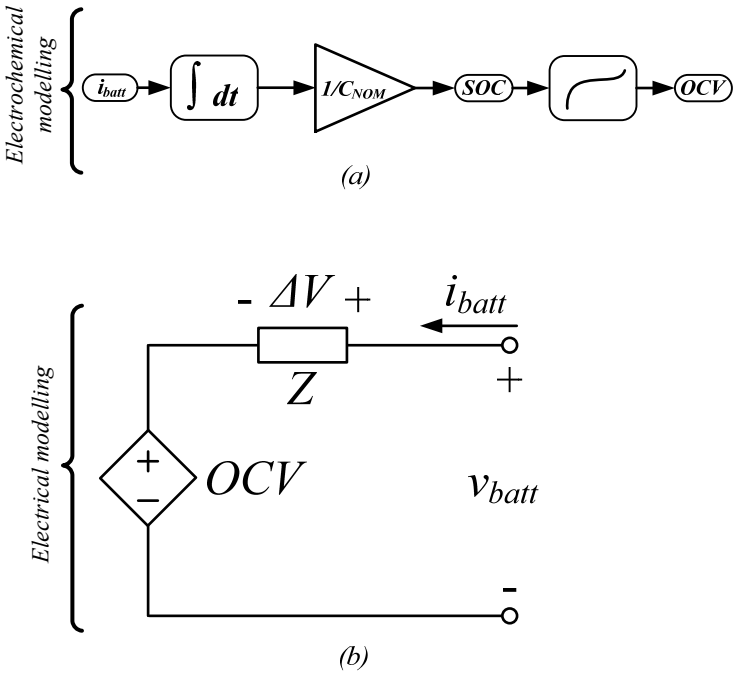

Fig. 1. Basic battery model. (a) Electrochemical modelling. (b) Electrical modelling

Using the impedance model of the battery and knowing the current, it is possible to determine the battery output voltage. Some studies introduce a complex impedance model: authors in [21] propose an asymmetric charge-discharge resistance, introducing RC tanks [22] and using One Time Constant (OTC) models (Fig. 2.a) or Two Time Constants models (TTC) (Fig. 2.b) [23], [24]. In order to model the self-discharge current, some studies add a resistor in parallel with the controlled voltage source *OCV*. This is the case when dealing with VRLA, whereas in lithium-based batteries it is not even considered. In this study, the OTC model is retained as a sufficient accuracy vs complexity compromise.

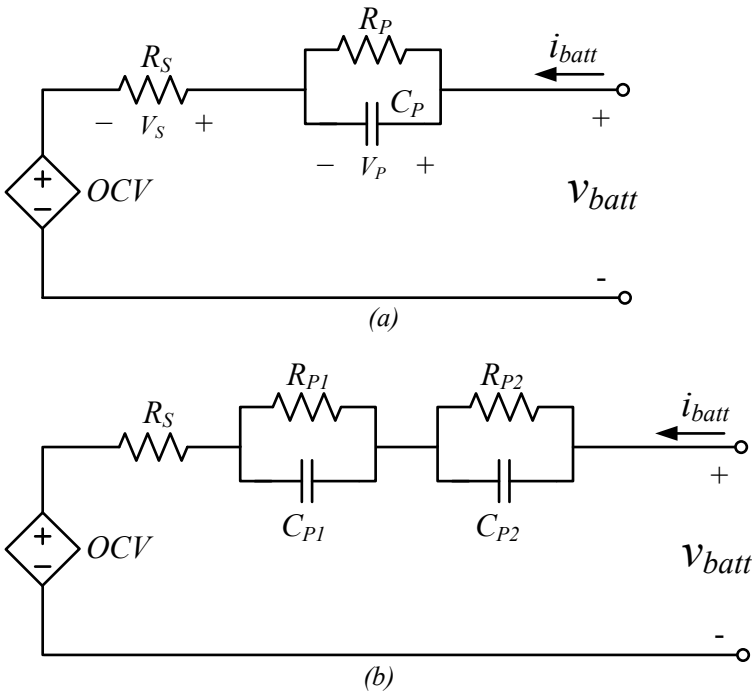

Fig. 2. (a) OTC impedance model. (b) TTC impedance model.

2.1.2. Underestimated effects

As it has been previously pointed out, there are some non-idealities that are not usually included in battery models but that must be considered:

- *Temperature effect in real time performance*. It is well-known that temperature influences battery performance, decreasing the maximum available capacity and the coulombimetric efficiency. The optimum operation conditions are reached around 20ºC. This effect varies with the chemistry technology, displaying different tendencies in Lead-Acid from Nickel-Cadmium or different types of Lithium [3], [16], [17]. The effects of varying temperature within the same charge-discharge cycle are not usually taken into account, but have a non-negligible impact in this application.

- *Incomplete charge process*. In regular laboratory tests, batteries are fully charged and discharged to evaluate their capacity, remaining several hours in bulk and float stages to ensure a complete charge. In off-grid PV applications, a complete cycle lasts just one day, and charge (insolation) hours may fluctuate considerably (depending on the season and latitude). Thus, a full-charge situation can never be assured. Due to this, the battery is always in an intermediate charge state. This is a less studied effect, but has proved to be as important as temperature, as it causes a further decrease in battery effective capacity.

Both effects together lead to a major reduction in actual available battery charge. This causes lower than expected charge reserve on typical days and can force a full battery discharge on a critically low sunlight day. It is paramount to take into account this behavior if an accurate simulation of the *SOC* evolution is desired.

It is not a simple task to incorporate these effects into a simulation model. As stated in (1), one of the parameters that define the *SOC* is C_{NOM}. Incorporating instant variations of this term (e.g. due to temperature) leads to instant variations of the *SOC* estimation, and to instant variations of the *OCV* term, both of which are not possible.

The typical test to measure this capacity consists in a full charge-discharge cycle, with several hours in floating state under a constant temperature. After that, C_{NOM} is established as the amount of Coulombs (or Ah) discharged in the process. In a photovoltaic installation, the charge process is limited by sunlight hours/radiation and is performed under variable temperatures. Thus, a battery cannot remain in the float stage for several hours, as in a manufacturer's tests and hence, the term C_{NOM} is not useful in modelling this application. Some studies [12], [25] reject the use of C_{NOM} and try to model its effects as a circuital non-linear bulk capacitance, but some temperature effects are left unmodelled if this approach is followed [13], [26].

The work presented here follows another approach based on a non-linear SS modelling and data-driven tests. How to incorporate these effects is explained in the following sections.

2.1.3. Thermal transport modelling

It is accepted that temperature has a great impact on battery performance. From a functional point of view, it influences in two ways:

- *Current integration speed*. Some studies [25], [27] support that temperature causes "current inefficiency", meaning that not all current is translated into charge.
- *Maximum storable charge*. From the same stored charge starting point, *OCV* grows faster in a colder battery, so it has stored less charge when it reaches float voltage.

The impact of temperature on battery performance has been traditionally addressed and measured in static exploration conditions. In other words, using the same temperature for the whole charge-discharge process. The results of the static temperature tests show that different operation temperatures cause a dramatic impact on battery capacity [3]. Example given, operating at a temperature 20ºC below the nominal temperature can lead to a 40-50% capacity drop in VRLA technologies. On the other hand, temperatures above the nominal one increase the effective capacity but, at the same time, they also increase the long term degradation that the battery undergoes.

When trying to integrate this effect in a model, capacity reduction caused by temperature makes Q, SOC and OCV no longer directly related as in the basic model. Q and OCV cannot be connected through simple functions, since colder and warmer batteries with the same measured C_{NOM} offer the same range of voltages in spite of their different storage capabilities [28].

In order to be able to model these situations it is necessary to modify the basic and accepted model of a fixed capacity. This modification is based on the following verified facts:

- OCV does not vary instantly as the result of a temperature change. It is its time derivative which does so [29] when current flows.
- Voltage rises and drops faster in a colder battery. This affects the maximum storable charge.
- As well as OCV, stored charge Q, does not vary instantly, but its time derivative does vary with the terminal current [11].
- Temperature affects the maximum storable charge while the battery is charging. Once it is charged, it has a lower impact [4] since practically all the stored charge may be drawn from it.

Some authors [11] propose dual SOC models in order to deal with capacity reduction issues when considering battery aging. To model the capacity reduction caused by temperature, the work presented here proposes a dual SOC model as well.

In order to differentiate the traditional SOC obtained by CC from that obtained through OCV, some additional definitions are required:

- Definition: SOC_V is the State-Of-Charge obtained using the OCV as a measure, instead of the CC method.
- Definition: C_{EX} represents the expected Capacity a battery shows instantly, when operating at different temperatures from the nominal. It is obtained by comparing Q against SOC_V, as in (3).

$$C_{EX} = \frac{Q}{SOC_V} \tag{3}$$

- Definition: $\eta_1(T)$ represents the current inefficiency coefficient, which models the impact of temperature on the current integration speed. It is a non-linear function that needs to be measured.
- Definition: $\eta_2(T)$ models the maximum capacity cap caused by temperatures different from the nominal temperature. It is also a non-linear function that needs to be measured or trained.

Thus, SOC_V and OCV have a one to one relationship as displayed in Fig. 3 (a) [11]. As happens with OCV, it is not this SOC_V which varies with temperature, but its time derivative.

In the basic model described in the previous section, only one state variable, Q, was needed since it was directly related to *SOC* and *OCV*. Once thermal fluctuations are introduced, there is a clear need to use two state variables, Q and *OCV*, as separate state variables. This is new and allows to model the desired effects. Therefore, a non-linear state-space approach can be considered to model this behavior. The equations are described as follows:

$$\frac{dQ}{dt} = f\left(i_{batt}, T\right) \tag{4}$$

$$\frac{dOCV}{dt} = f\left(OCV, Q, i_{batt}, T\right) \tag{5}$$

Equation (4) can be developed using the current efficiency described previously:

$$\frac{dQ}{dt} = \eta_1(T) \cdot i_{batt} \tag{6}$$

Equation (5) can also be developed, relating *OCV* to SOC_V as in (7). The term $\eta_2(T)$ which modifies the expected capacity, can be introduced in (8):

$$\frac{dOCV}{dt} = \frac{dOCV}{dSOC_V} \cdot \frac{dSOC_V}{dt} \tag{7}$$

$$\frac{dSOC_V}{dt} = \frac{i_{batt}}{\frac{C_{ex}}{\eta_2(T)}} = \eta_2(T) \cdot \frac{i_{batt} \cdot SOC_V}{Q} \tag{8}$$

As hypothesized, *OCV* and SOC_V maintain a one-to-one non-linear relationship, so (9) and (10) can be established.

$$SOC_V \triangleq f_1(OCV) \tag{9}$$

$$\frac{dOCV}{dSOC_V} \triangleq f_2(OCV) \tag{10}$$

Replacing (8), (9), and (10) into (7), the final non-linear state equation for *OCV* can be achieved:

$$\frac{dOCV}{dt} = \frac{i_{batt}}{Q} \cdot \eta_2(T) \cdot f_1(OCV) \cdot f_2(OCV) \tag{11}$$

There are four non-linear functions, $\eta_1(T)$, $\eta_2(T)$, $f_1(OCV)$ and $f_2(OCV)$ which are to be either measured or estimated. Fig. 3.a describes the relationship between *OCV* and SOC_V as an injective function, $f_1(OCV)$ defined as in (9) can be determined as its

inverse function and $f_2(OCV)$, as its derivative (Fig. 3.b, c). The temperature-dependent functions $\eta_1(T)$, $\eta_2(T)$ and how to measure them, will be discussed further on.

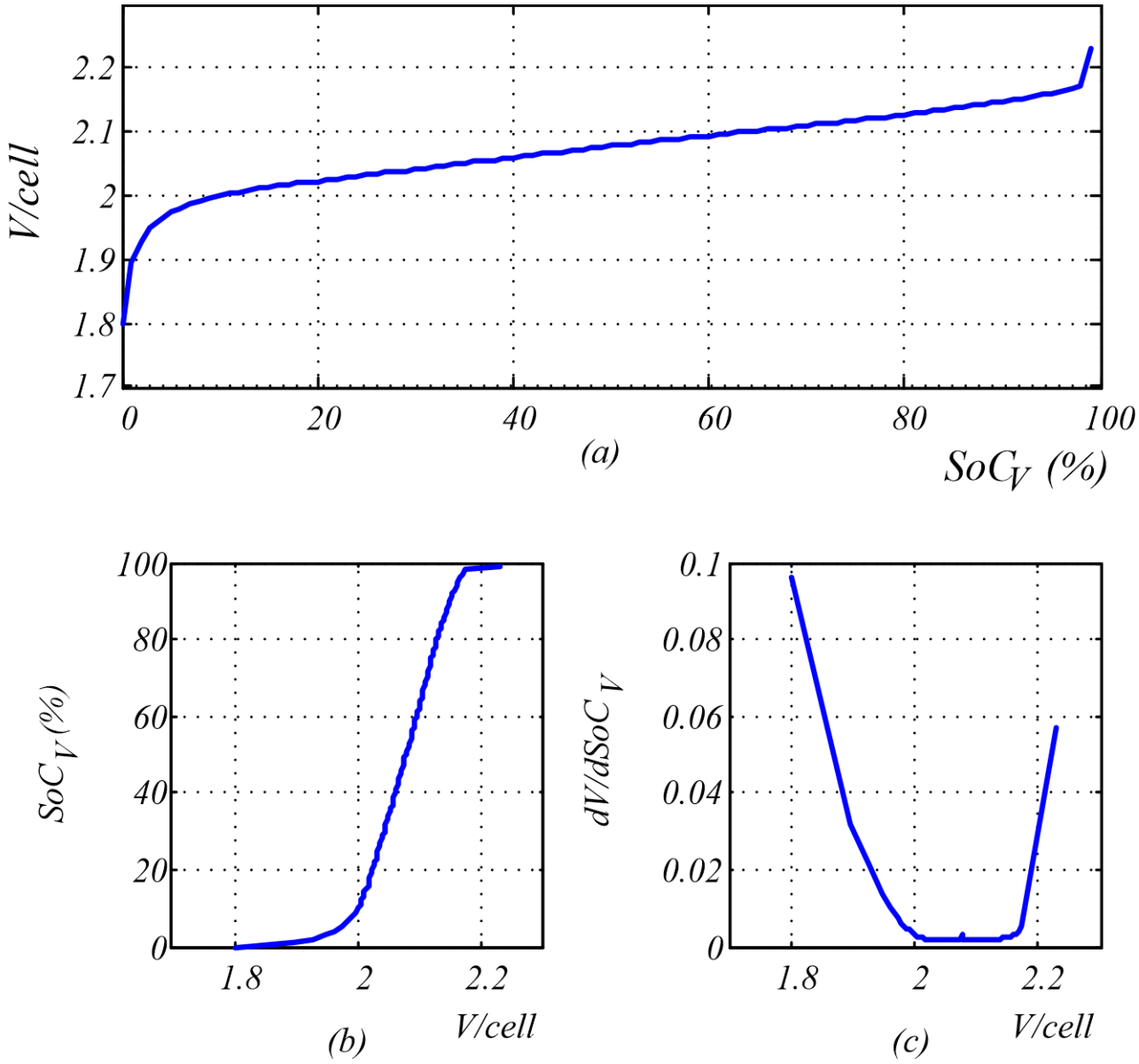

Fig. 3. (a) OCV-SOCv Curve. (b) Inverse curve. (c) Derivative curve.

2.1.4. Partial charge modelling

In some other battery applications such as EV, or in capacity measuring tests, charge processes may take as long as necessary. The battery may remain in floating stage or equalizing stage for several hours, until it can be considered fully charged. The batteries under study, for example, must remain in float stage at 2,23V/cell for 72 hours to be considered at full charge, according to the manufacturer's indications. The use of higher float voltages may shorten this period of time, but never below 24h in floating phase.

In a PV installation, charge hours rely only on insolation. Thus, a battery can never remain in float stage for 72h (so it can never be considered fully charged). A typical current pattern is shown in Fig. 4.a. Due to this natural limitation during the insolation hours, the battery never reaches its full charge state and remains in a partial charge state, decreasing the available energy at critical periods of time (Fig. 4.b).

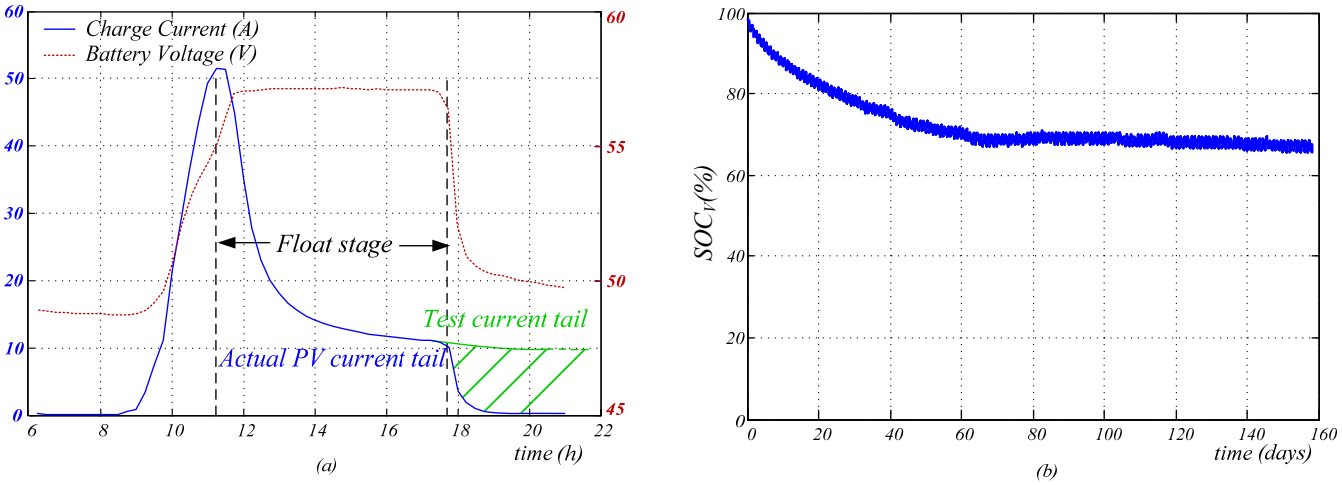

Fig. 4. (a) Average PV charge pattern. (b) Partial SOC_V reached with this pattern.

There are two main parameters within the model that define the current tail that appears in the float stage, which are the curve that associates SOC_V with OCV, and the aggregate electric impedance that the system offers (the addition of the internal battery impedance and the installation parasitic resistance). A battery can be modeled as a non-linear capacitance [30], [31] with a very high storage capacity. Though its internal voltage varies non-linearly with the charge it stores, this effect can be explained using a simple RC equivalent circuit under constant voltage. A higher ESR limits the peak current tail in float stage, decreasing the amount of charge stored in this period of time and extending the current tail throughout time. A small ESR allows a higher peak current, helping the battery to reach the minimum tail sooner (ideally zero).

As explained, in order to capture partial charge effects, there is a clear need for battery impedance characterization. Among all impedance modelling options found in state of the technique, this study considers the OTC model (Fig. 2 (a)) as an initial approach to the impedance modelling.

This circuital model can be included into the SS model, using equation (12).

$$\frac{dV_P}{dt} = \frac{1}{C_P} \cdot i_{C_P} = \frac{1}{C_P}\left(i_{batt} - \frac{V_P}{R_P}\right) \qquad (12)$$

Hitherto, the equations have described the state variables, but the inputs and the outputs to the system have not been discussed. When the battery is working in the current regulation phase, the charger fixes i_{batt}, and v_{batt} acts as an output of the model (13):

$$v_{batt} = OCV + i_{batt} \cdot R_S + V_P \tag{13}$$

However, when the v_{batt} reaches the float voltage, the charger changes to Voltage Regulation Phase, and so v_{batt} is fixed and represents an input to the system, and the battery chooses i_{batt}. The current can be calculated as an output of the SS system (14):

$$i_{batt} = \frac{V_S}{R_S} = \frac{v_{batt} - V_P - OCV}{R_S} \tag{14}$$

The method to obtain the parameters R_S, R_P and C_P will be discussed later.

2.1.5. Complete model

Taking into account these effects, which are usually not considered, and making use of the SS modelling, this study proposes the complete model described by the following state equations (15). The state variables are OCV, Q and V_P.

$$\begin{cases} \dfrac{dQ}{dt} = \eta_1(T) \cdot i_{batt} \\ \dfrac{dOCV}{dt} = \dfrac{i_{batt}}{Q} \cdot \eta_2(T) \cdot f_1(OCV) \cdot f_2(OCV) \\ \dfrac{dV_P}{dt} = \dfrac{1}{C_P}\left(i_{batt} - \dfrac{V_P}{R_P} \right) \end{cases} \tag{15}$$

For simulation purposes, an external element is required (simulating the battery charger or solar regulator) that models the battery charge policy. This element switches between both control modes (Current Regulation Mode, Voltage Regulation Mode) e.g. when the desired float voltage is reached, or when insolation hours end and discharge starts.

3. Results and discussion

3.1. Model Training

The usual procedure when sizing battery installations is to consult the manufacturer's catalogue and datasheet. The information they provide, such as aging consequences or the impact of temperature in capacity, comes from normalized laboratory tests, in which batteries are subjected to full charge-discharge tests, and thus, capacity is defined. For instance, low temperature impact is addressed as a reduction in the battery capacity [3], [16]. A first approach to train the model could be

to use this data for this purpose. This straightforward approach is not suitable when considering intra-cycle temperature variations.

In order to train the model, battery tests have been performed. These are described in the following sections and the test bench used for these measures is displayed in Fig. 5.a. It consists of a climatic chamber (A), where the batteries (B) are kept, and an *ad hoc* designed battery cycler (C), which can act as a power source or a power sink, and controls how the batteries are charged or discharged (Fig. 5.b). Both of them can be controlled from a PC (D) using MatLab software and a communication protocol. Other elements such as a multimeter (E) or an oscilloscope are also used in the test bench.

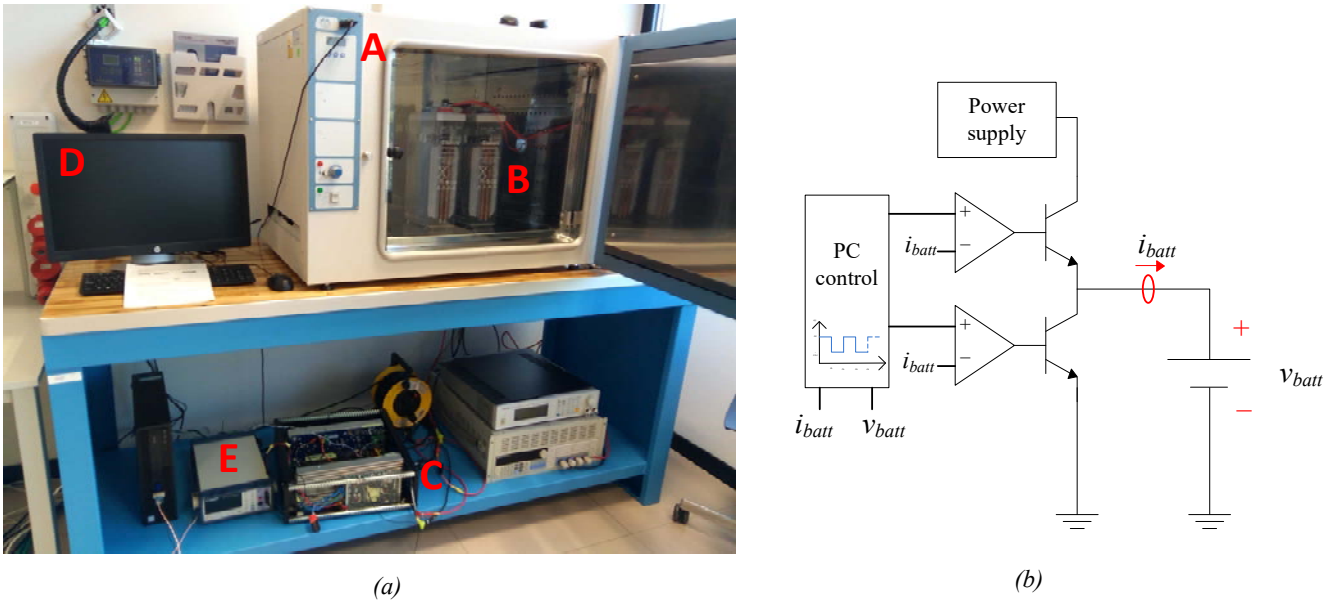

(a) *(b)*

Fig. 5. (a)Test bench. (b) *ad hoc* battery cycler scheme

The test parameters are displayed in Table 1.

Table 1. Discharge test features

Battery cell	*Exide OPzS Solar*
Nominal Capacity [Ah]	*190*
Nominal Voltage [V]	*2*
Number of cells	*2*
Nominal Temperature [ºC]	*25*
Multimeter	*BK PRECISION 5491B*
Power supply	*PM3006-2*
Oscilloscope	*TEKTRONIX TD57104*
Climatic chamber	*Prebatem 2000962*
Battery Cycler	*Ad-hoc cycler*

3.1.1. Temperature fitting

As the new model being considered differs from the traditional use of capacity, a new laboratory temperature test must be designed. As a result of the analysis of temperature patterns in a Spanish continental climate, where the studied *PV* installations are located, three temperatures have been established as references to conduct laboratory tests. Specifically, these test temperatures are:

- 25ºC. Used as nominal temperature, where the battery performs as expected by datasheet.
- 5ºC. Used as a cold reference temperature.
- 35ºC. Used as a hot reference temperature.

In order to capture the thermal transport effect, cross-temperature charge-discharge cycles will be performed. This means that the tests are designed to separate the temperature influence during the charge process, from the influence during the discharge process. The tests consist of a charge process with several hours in float stage at the selected charge temperature, followed by a full-discharge process at the selected discharge temperature. Following the tests, the previously introduced efficiency coefficients $\eta_1(T)$ and $\eta_2(T)$ may be determined.

The results of the cross-temperature Coulomb efficiency are displayed in Table 2. This efficiency is related to the reference cycle (charge at 25ºC, discharge at 25ºC). From these results, $\eta_1(T)$ and $\eta_2(T)$ can be estimated.

Table 2. Cross-temperature efficiency results

Charge Temperature	Discharge temperature	Coulomb Efficiency
5ºC	5ºC	*-34.7%*
25ºC	5ºC	*-12%*
	35ºC	*+5%*
35ºC	35ºC	*+16.4%*

The *OCV* factor, $\eta_2(T)$, is not directly obtainable due to the non-linear functions within the model. It modifies the maximum storable charge when charging at different temperatures. However, if the batteries have been charged at the same temperatures, the Q term compensates the temperature impact, and it has no effect on the outcome. Thus, the differences in the Coulomb Efficiencies in the cycles (charge at 25ºC; discharge at 5ºC) and (charge at 25ºC; discharge at 35ºC) are caused by the $\eta_1(T)$ coefficient. These coefficients are linear with the stored charge Q (they directly modify i_{batt}). Therefore, these can be directly extracted from Table 2.

Once $\eta_1(T)$ coefficients are added to the model, there is a training process, in which the $\eta_2(T)$ function needs to be estimated. By using optimization methods in such a way that the coulomb efficiency obtained by the model matches that gathered by the tests, the coefficients may be obtained, and the temperature model will be fully accomplished.

3.1.2. Partial Charge modelling

As stated, modelling the internal impedance of the battery is necessary, intending to imitate the behavior it features in voltage mode, when the charger sets the float voltage to the battery. To achieve this, a more complex impedance model needs discussing, and specific tests performing. One time constant (OTC) models feature a good compromise between accuracy and complexity.

Therefore, there are three electrical parameters to be applied to the electrical model, as well as the relationship between *SOC* and *OCV*, which links the electrochemical model and the electrical model. In order to do so, specific lab tests need to be designed. The Hybrid Power Pulse Characterization (HPPC) test as described in *IEC 62600-1* is a common test used for this purpose. It uses fast discharge pulses and lets the battery evolve, to determine the time constants of its response. In [20], [32], a variation of this test is proposed. It applies fast discharge pulses and then the battery is allowed to rest, to measure its *OCV*. This process is repeated until the battery is completely discharged. This test has been followed to measure the electrical parameters in Fig. 2. The waveforms of the test are displayed in Fig. 6.a.

The electrical parameters are measured as follows. First, the battery must be heated up to 25ºC, charged up to its float voltage, and must remain in float stage for at least 72h. After that period of time, v_{batt} and *OCV* can be assumed to be equal.

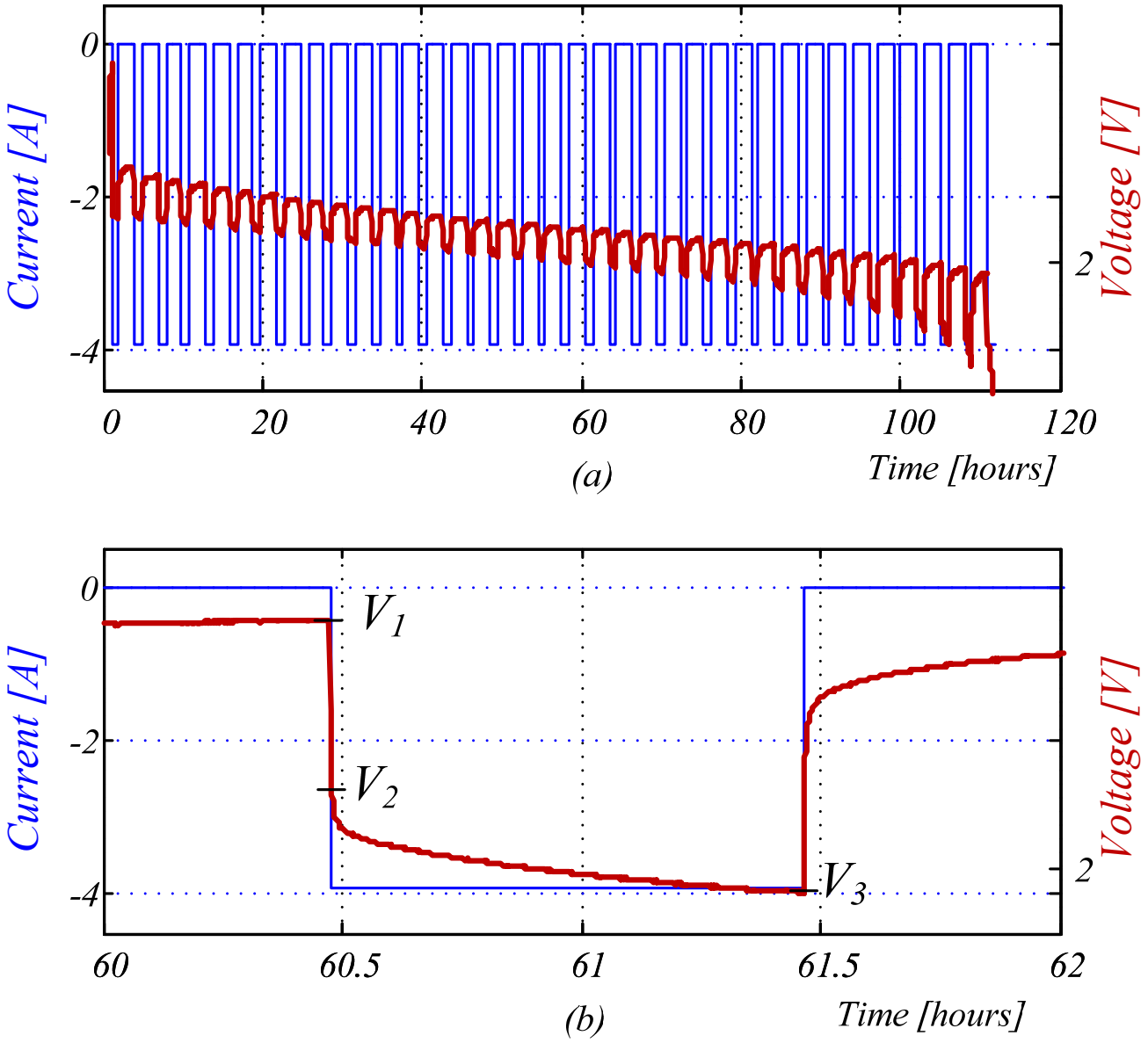

Fig. 6. (a) Current and voltage test waveforms. (b) Zoom in the same curve.

The short-term dynamic is modeled by the RC tank. In one of the current pulses, these parameters and the series resistance R_S can be determined, as shown in Fig. 6.b. The difference between V_1 and V_2 is the contribution of the resistance R_S, and the difference between V_2 and V_3 is the contribution of the resistance R_P, once the transient response is stable. Measuring the time constant of this transient response, C_P can be determined. These parameters may vary with the SOC_V [27] but in the operation region (60 to 70% of SOC_V, Fig. 4.b) they remain steady. Their values are collected in Table 3.

Table 3. OTC model measured parameters

Parameter	Value at *60-70% SOC_V*
R_S	*47 mΩ*
R_P	*18 mΩ*
C_P	*$1.1x10^4 F$*

The complete model is now ready for its implementation using software tools. In this case, the forthcoming simulations are to be developed using Matlab/Simulink software. To this purpose, an implementation of the formerly described state-space model has been implemented, and fed with the data and processes described in this section.

3.2. Model Validation

3.2.1. Temperature validation

In order to validate the model behavior in term of temperature changes throughout the charge and discharge processes, the model has been compared with laboratory and experimental tests. To this purpose, real batteries have been charged at different temperatures using climate chambers, and then discharged at other temperatures. Fig. 7 shows some of these tests: the evolution of the battery voltage and the model voltage in the three different discharge temperatures: 5ºC, 25ºC and 35ºC after a full-charge process at 25ºC.

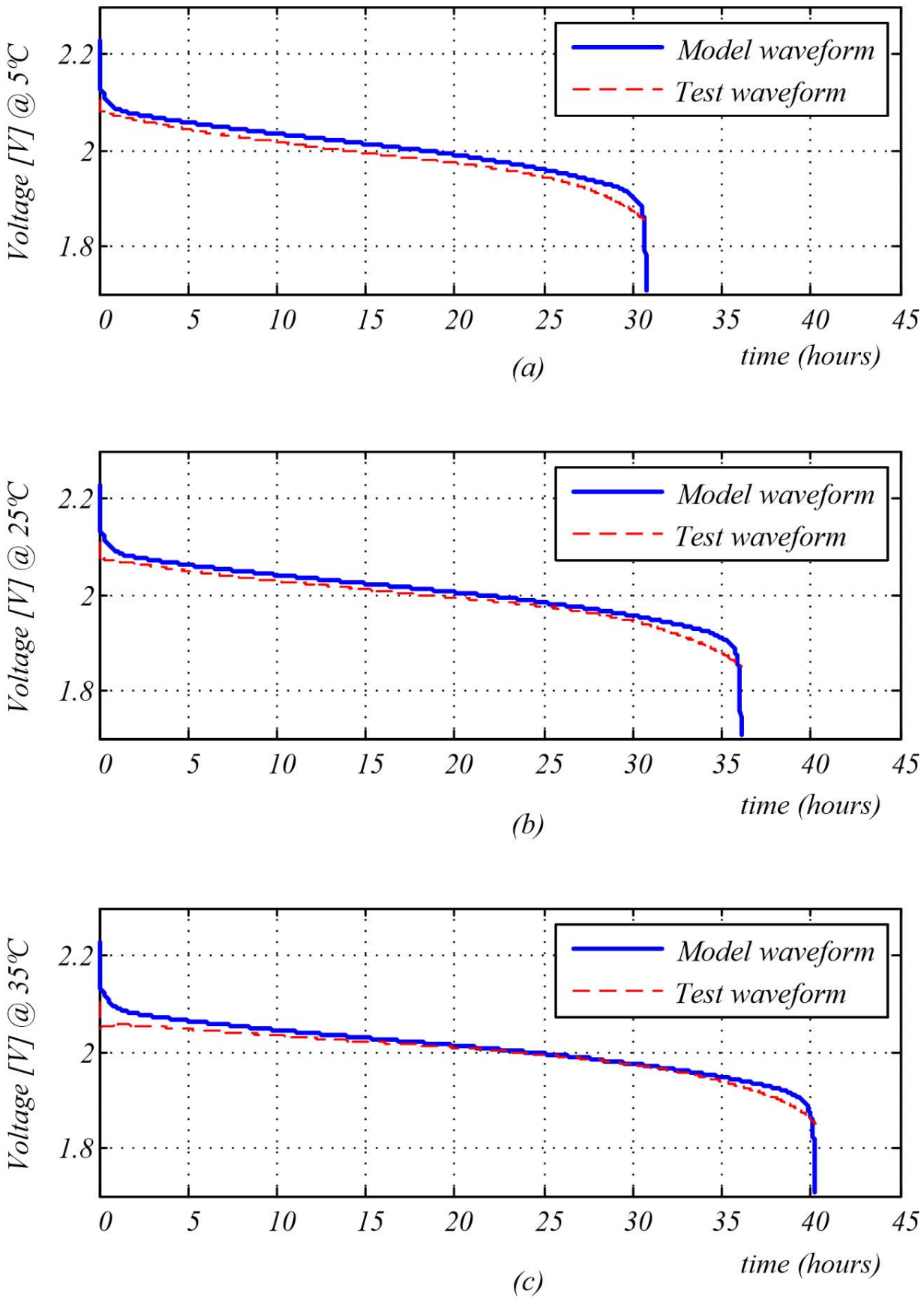

Fig. 7. Voltage waveforms at different temperatures: (a) 5ºC. (b) 25ºC. (c) 35ºC

As shown, the model performs in good agreement with the measured data, replicating correctly the discharge process at the different chosen temperatures.

3.2.2. Remaining charge after partial cycling process

The model and a real battery are tested under the same cycling conditions, to check that the model is capable of correctly estimating the remaining charge inside the battery. After an exhaustive study of the PV installations being considered, a test current pattern has been established. This pattern consists of 100 charge-discharge cycles, with the same features of 100 complete PV sunny cycles. After the cycles, the real batteries were fully discharged, in order to obtain the available charge in the battery (incomplete charge). See Table 4.

Table 4. Remaining charge after 100 solar-like cycles

Temperature	Real battery	Model
5ºC	16 Ah	53 Ah
25ºC	75 Ah	76 Ah
35ºC	93 Ah	89 Ah

As shown, the model presents a good match with the laboratory data, reaching similar charge levels after the 100-cycle test at the higher temperatures (25ºC, 35ºC). However, at the lowest temperature, test voltage drops quicker, and the amount of extracted charge is minute. This could be caused by an impedance model that varies with temperature.

3.2.3. Comparison against real off-grid PV patterns

To extend the model soundness in the PV application, it has been tested with real current and voltage patterns from real PV installations. Fig. 8.a, b shows how the discharge voltage is correctly estimated during weekly intervals, using real measured patterns of the summer of 2009 in PV installations. Although the discharge voltage is well estimated, some inaccuracies can be seen, especially when it comes to estimating voltage during charge hours.

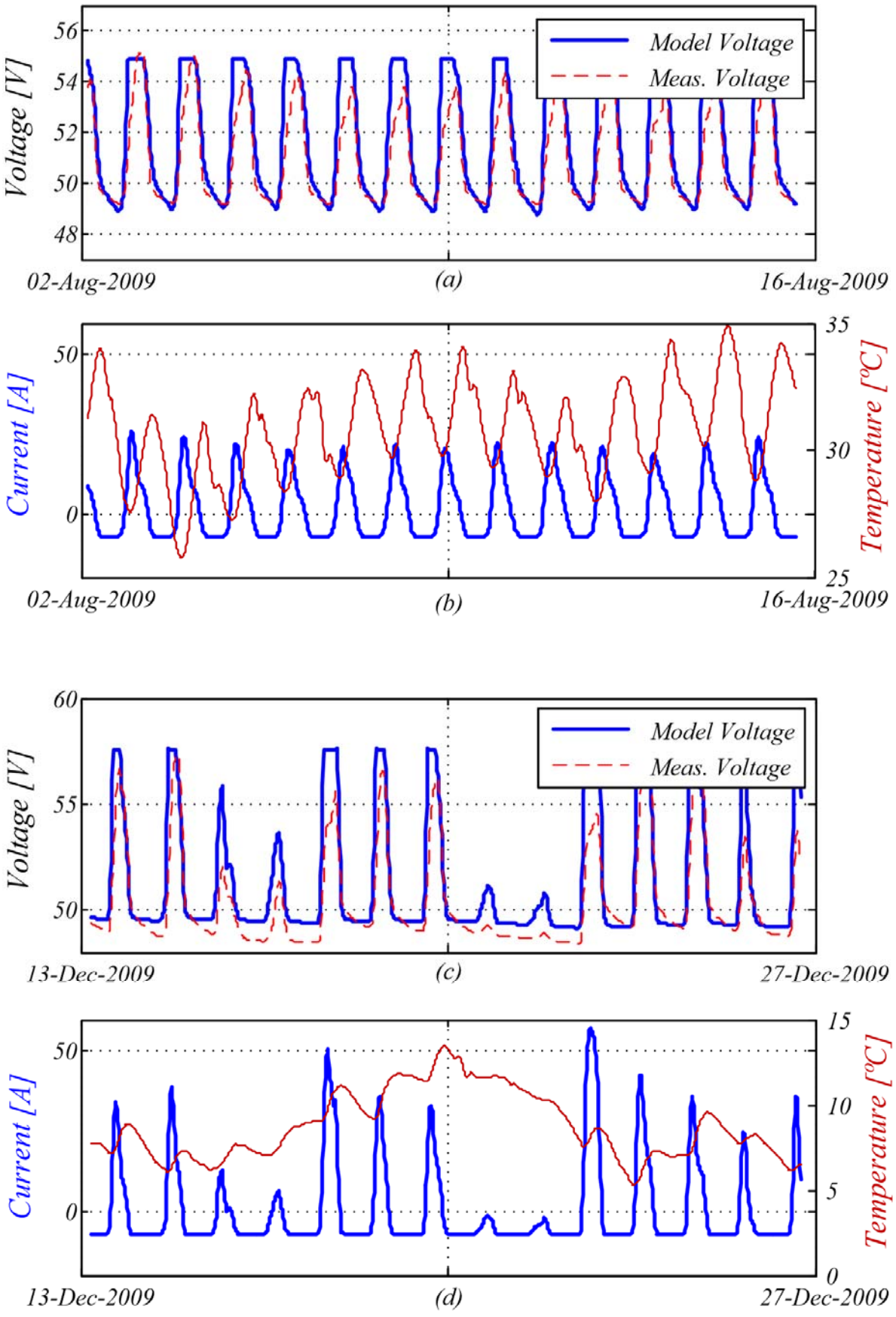

Fig. 8. (a), (b) Voltage, current and temperature waveforms in summer. (c), (d) winter.

It seems that the model tends to overestimate the voltage when receiving positive current. This may be caused by the single impedance model, and strengthens the theory of an asymmetric impedance [21].

Besides this effect, the model presents some inaccuracy when trying to estimate discharge voltage at low temperatures e.g. winter nights (Fig. 8 (c), (d)). Again, this effect can be modeled using a temperature-dependent impedance model, as proposed in [33].

4. Conclusions

Energy Storage Systems used in standalone off-grid PV applications suffer from the specific charge conditions of these installations. Their batteries suffer from intra-cycle temperature variations, which are not modelled in typical constant temperature researches/datasheets/app notes, and usually remain in an intermediate *SOC* due to the nature of the incomplete charge-discharge cycles in this kind of application. These effects provide an effective decrease in the battery stored charge, and in many cases, they are omitted.

This paper presents a novel simulation model for batteries specifically used in this kind of applications. The model described unifies both effects and makes it possible to replicate them, defining the traditionally associated *OCV* and *Q* as two different state variables. This approach models dynamic capacity reduction caused by temperature changes. An OTC electric model is used to capture the differences between the *OCV* and the voltage at the battery terminals.

The model performs accurate estimations of the remaining charge inside a battery after the partial charge stationary effect. Manufacturers do not give any data on this effect which causes a considerable decrease in the available stored charge at a certain moment. The relative error that the model performs is below 2% at nominal temperatures, and below 5% at higher temperatures. At lower temperatures, the measurement of error grows. Therefore, as a future improvement, the model will be enhanced by adding a temperature-dependent impedance characterization.

This new methodology has also been tested with real measure data from PV sites. The results show that the model also replicates voltage and remaining charge during the discharge process in summer periods, but differs from the actual voltage during the charge process, or during winter period. Again, to this purpose, the impedance model can be enhanced, adding a temperature-dependent model, or making it asymmetrical with the input current. This will be the scope of future researches.

Forthcoming generations of ESSs will have the capability of managing energy in many different energy packs, using different storage technologies and adapting them to their best use. They will need of accurate available charge prediction in order to have successful energy management policies.

Acknowledgements

The authors want to acknowledge the support from MINECO RTC-2015-3358-5 project and FEDER funding from the Spanish government and European Union, and the support from Sociedad Ibérica de Construcciones Eléctricas S.A.

References

[1] G. J. May, "Recent progress in the development of VRLA batteries for the global telecom market," in *Proceedings of Intelec'96 - International Telecommunications Energy Conference*, pp. 168–171.

[2] S. S. Misra and A. J. Williamson, "On temperature compensation for lead acid batteries in float service: its impact on performance and life," in *Proceedings of Intelec'96 - International Telecommunications Energy Conference*, pp. 25–32.

[3] Exide Technologies, "Handbook for Stationary Vented Lead-Acid Batteries Part 2 : Installation , Commissioning and Operation," vol. 2, pp. 1–68, 2012.

[4] E. Garayalde, I. Aizpuru, J. M. Canales, I. Sanz, C. Bernal, and E. Oyarbide, "Análisis Experimental del Efecto de la Temperatura y la Tensión de Carga para la Optimización Energética de Sistemas de Almacenamiento de Instalaciones Fotovoltaicas Aisladas," *SAAEI 2017*, 2017.

[5] L. Lu, X. Han, J. Li, J. Hua, and M. Ouyang, "A review on the key issues for lithium-ion battery management in electric vehicles," *J. Power Sources*, vol. 226, pp. 272–288, 2013.

[6] P. Thounthong, S. Raël, and B. Davat, "Energy management of fuel cell/battery/supercapacitor hybrid power source for vehicle applications," *J. Power Sources*, vol. 193, pp. 376–385, 2009.

[7] M. G. Carignano, R. Costa-Castell O, V. Roda, N. M. Nigro, S. Junco, and D. Feroldi, "Energy management strategy for fuel cell-supercapacitor hybrid vehicles based on prediction of energy demand," *J. Power Sources*, 2017.

[8] W. L. Burgess, "Valve Regulated Lead Acid battery float service life estimation using a Kalman filter," *J. Power Sources*, vol. 191, no. 1, pp. 16–21, 2009.

[9] M. A. Hannan, H. Lipu, A. Hussain, and A. Mohamed, "A review of lithium-ion battery state of charge estimation and management system in electric vehicle applications: Challenges and recommendations," *J. Power Sources*, 2017.

[10] X. Tang, B. Liu, and F. Gao, "State of charge estimation of LiFePO 4 battery based on a gain-classifier observer," *Energy Procedia*, vol. 105, pp. 2071–2076, 2017.

[11] S. Tong, M. P. Klein, and J. W. Park, "On-line optimization of battery open circuit voltage for improved state-of-

charge and state-of-health estimation," *J. Power Sources*, vol. 293, pp. 416–428, 2015.

[12] M. Shahriari and M. Farrokhi, "Online state-of-health estimation of VRLA batteries using state of charge," *IEEE Trans. Ind. Electron.*, vol. 60, no. 1, pp. 191–202, 2013.

[13] S. Piller, M. Perrin, and A. Jossen, "Methods for state-of-charge determination and their applications," *J. Power Sources*, vol. 96, no. 1, pp. 113–120, 2001.

[14] A. H. Anbuky and P. E. Pascoe, "VRLA battery state-of-charge estimation in telecommunication power systems," *IEEE Trans. Ind. Electron.*, vol. 47, no. 3, pp. 565–573, Jun. 2000.

[15] P. E. Pascoe and A. H. Anbuky, "VRLA battery discharge reserve time estimation," *IEEE Trans. Power Electron.*, vol. 19, no. 6, pp. 1515–1522, 2004.

[16] Saft Batteries, "Sunica.plus Technical manual," 2007.

[17] Saft Batteries, "Nickel-cadmium batteries for telecom networks," 2004.

[18] B. S. Bhangu, P. Bentley, D. A. Stone, and C. M. Bingham, "Nonlinear Observers for Predicting State-of-Charge and State-of-Health of Lead-Acid Batteries for Hybrid-Electric Vehicles," *IEEE Trans. Veh. Technol.*, vol. 54, no. 3, pp. 783–794, May 2005.

[19] K. S. Ng, C.-S. Moo, Y.-P. Chen, and Y.-C. Hsieh, "Enhanced coulomb counting method for estimating state-of-charge and state-of-health of lithium-ion batteries," *J. Power Sources*, 2009.

[20] M. Chen and G. A. Rincon-Mora, "Accurate Electrical Battery Model Capable of Predicting Runtime and I–V Performance," *IEEE Trans. Energy Convers.*, vol. 21, no. 2, pp. 504–511, Jun. 2006.

[21] M. Coleman, C. K. Lee, C. Zhu, W. G. W. G. Hurley, C. K. Chi Kwan Lee, C. Chunbo Zhu, W. G. W. G. Hurley, C. K. Lee, C. Zhu, and W. G. W. G. Hurley, "State-of-charge determination from EMF voltage estimation: Using impedance, terminal voltage, and current for lead-acid and lithium-ion batteries," *IEEE Trans. Ind. Electron.*, vol. 54, no. 5, pp. 2550–2557, Oct. 2007.

[22] S. Cho, H. Jeong, C. Han, S. Jin, J. H. Lim, and J. Oh, "State-of-charge estimation for lithium-ion batteries under various operating conditions using an equivalent circuit model," *Comput. Chem. Eng.*, vol. 41, pp. 1–9, 2012.

[23] A. Rahmoun, H. Biechl, and A. Rosin, "Evaluation of Equivalent Circuit Diagrams and Transfer Functions for Modeling of Lithium-Ion Batteries," *Electr. Control Commun. Eng.*, no. 2, 2013.

[24] M. Dubarry and Y. Liaw, “Development of a universal modeling tool for rechargeable lithium batteries,” *J. Power Sources*, vol. 174, pp. 856–860, 2007.

[25] V. H. Johnson, A. A. Pesaran, and T. Sack, “Temperature-Dependent Battery Models for High-Power Lithium-Ion Batteries,” 2000.

[26] S. Barsali and M. Ceraolo, “Dynamical Models of Lead-Acid Batteries: Implementation Issues,” *IEEE Trans. ENERGY Convers.*, vol. 17, no. 1, 2002.

[27] S. Sepasi, R. Ghorbani, and B. Y. Liaw, “Inline state of health estimation of lithium-ion batteries using state of charge calculation,” *J. Power Sources*, vol. 299, pp. 246–254, 2015.

[28] M. Ceraolo, “New dynamical models of lead-acid batteries,” *IEEE Trans. Power Syst.*, vol. 15, no. 4, pp. 1184–1190, 2000.

[29] T. Kim, Y. B. Wang, Z. Sahinoglu, T. Wada, S. Hara, and W. Qiao, “State of Charge Estimation Based on a Real-time Battery Model and Iterative Smooth Variable Structure Filter,” *2014 Ieee Innov. Smart Grid Technol. - Asia (Isgt Asia)*, pp. 132–137, 2014.

[30] Z. M. Salameh, M. A. Casacca, and W. A. Lynch, “A mathematical model for lead-acid batteries,” *IEEE Trans. Energy Convers.*, vol. 7, no. 1, pp. 93–98, Mar. 1992.

[31] P. M. Hunter and A. H. Anbuky, “VRLA Battery Virtual Reference Electrode: Battery Float Charge Analysis,” *IEEE Trans. Energy Convers.*, vol. 23, no. 3, pp. 879–886, Sep. 2008.

[32] B. S. Bhangu, P. Bentley, D. a. Stone, and C. M. Bingham, “State-of-charge and state-of-health prediction of lead-acid batteries for hybrid electric vehicles using non-linear observers,” *2005 Eur. Conf. Power Electron. Appl.*, pp. 1–10, 2005.

[33] L. W. Juang, P. J. Kollmeyer, T. M. Jahns, and R. D. Lorenz, “Improved modeling of lithium-based batteries using temperature-dependent resistance and overpotential,” in *2014 IEEE Transportation Electrification Conference and Expo (ITEC)*, 2014, pp. 1–8.